Synthesis and Hybridization Properties of Thiazolidine PNAs

Sarah Bregant,[a] Fabienne Burlina,[a] Jacqueline Vaissermann,[b] and Gérard Chassaing*[a]

Keywords: DNA recognition / Peptide nucleic acids / Sulfur heterocycles

Two new, constrained PNA monomers, each containing a thiazolidine ring, were synthesized and incorporated into a central position in a PNA. It was shown by UV melting experiments that the presence of a single constrained unit does not prevent the cooperative association of the PNA but does significantly destabilize PNA/DNA and PNA/RNA triplexes.

Introduction

Since their introduction in 1991 by Nielsen et al.,[1] Peptide Nucleic Acids (PNAs) have reenergized the area of antisense and antigene strategies and have found applications as tools in molecular biology and genetic diagnostics.[2] PNAs are DNA mimics in which the nucleobases are attached by means of a methylenecarbonyl linker to an achiral and neutral polyamide backbone composed of *N*-(2-aminoethyl)glycine (**aeg**) units (Figure 1, **A**). These polymers are resistant to cellular nucleases and proteases, and bind to DNA and RNA with higher sequence specificity and affinity than unmodified oligonucleotides do. However, application of PNAs as gene targeting agents is limited by their low aqueous solubility, poor cellular uptake and ambiguity in their binding orientations to nucleic acids.[3] Many chemical modifications to improve PNAs' properties, recently reviewed by Ganesh et al.,[4] have been proposed. Some of these modifications involve the rigidification of the PNA backbone (by cyclisation of the monomeric units) to favour the structure observed in PNA/DNA or PNA/RNA complexes and improve hybridization properties. Those conformationally constrained PNAs that have been reported can be classified into five groups, depending on the restrained torsion angles (Figure 1):

- β (cyclohexyl PNA),[5]
- β, γ and δ (4-aminoprolyl PNA),[6,7]
- δ, χ_1 and χ_2 [*N*-(2-aminoethyl)propyl PNA],[8]
- γ, χ_1 and χ_2 (pyrrolidine[9] and pyrrolidinone[10] PNAs)
- γ, δ, χ_1 and χ_2 (glycyl prolyl PNA).[7,11]

Enhanced DNA affinity has been obtained with 4-aminoprolyl-PNA, *N*-(2-aminoethyl)propyl-PNA and pyrrolidine PNA. On the basis of analyses of the aegPNA complexes' structures,[12] we have designed two novel constrained PNA units, each containing a thiazolidine ring, which restrains the fluctuation domain of the γ and δ torsion angles (Figure 1, **B**). The *anti*-(aminomethyl)thiazolidine unit mimics the γ and δ torsion angle values observed in the aegPNA/DNA, aegPNA$_2$/DNA and aegPNA/RNA complexes. In contrast, the γ and δ torsion angle values obtained with the *syn*-(aminomethyl)thiazolidine unit are observed only in the aegPNA/DNA duplexes. Thiazolidine rings have been exploited in several areas of chemistry: as masked aldehydes in peptide chemistry,[13] as pseudo-prolines to promote peptide solubilization during solid-phase synthesis[14] or to constrain peptide bonds,[15] as scaffolds in combinatorial chemistry,[16] and also as building blocks in the synthesis of biotin.[17] Thiazolidines are generally obtained by condensation of (β-mercaptoalkyl)amines with aldehydes and ketones. This introduces an additional chiral centre, the stereochemistry of which is difficult to control. In this paper, we report the novel syntheses of the (2*S*,4*R*) and (2*R*,4*R*) diastereomers of 2-(aminomethyl)-3-(thyminylacetyl)thiazolidine-4-carboxylic acid. Incorporation of the constrained monomers into a PNA sequence by solid-phase synthesis

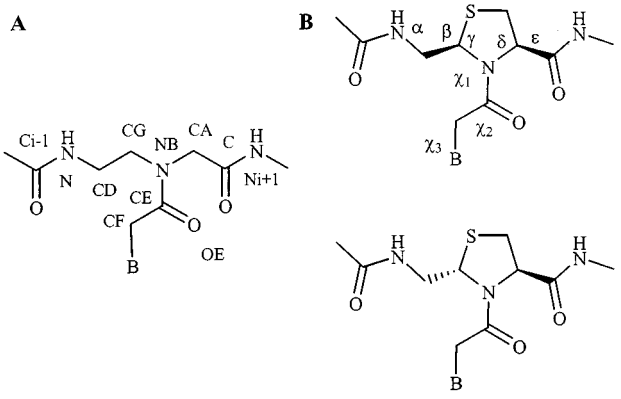

Figure 1. Structure of the PNA units with dihedral angle and atom nomenclature; the atom labelling convention of Betts et al. is used;[25b] torsion angles: α: C_{i-1}-N-CD-CG; β: N-CD-CG-NB; γ: CD-CG-NB-CA; δ: CG-NB-CA-C; ε: NB-CA-C-N_{i+1}; χ_1: CG-NB-CE-CF; χ_2: NB-CE-CF-N1(pyr); χ_3: CE-CF-N1(pyr)-C2(pyr) (pyr = pyrimidine); **A**: *N*-(2-aminoethyl)glycine unit (**aeg** units); **B**: *syn*- and *anti*-(aminomethyl)thiazolidine units (**amt** units)

[a] Laboratoire de Chimie Structurale Organique et Biologique, Université P. et M. Curie, CNRS UMR 7613
4 place jussieu, 75252 Paris Cedex 05, France
Fax: (internat.) + 33-1/44273783
E-mail: chassain@ccr.jussieu.fr
[b] Laboratoire de Chimie Inorganique et Matériaux Moléculaires, Université P. et M. Curie, CNRS ESA 7071
4 place jussieu, 75252 Paris Cedex 05, France
Fax: (internat.) + 33-1/44273841
E-mail: java@ccr.jussieu.fr

  1434−193X/01/0917−3285 $ 17.50+.50/0

and hybridization studies with DNA and RNA are also presented.

Results and Discussion

Synthesis of the (Aminomethyl)thiazolidine PNA Monomers

The syntheses of the *syn*- and *anti*-(aminomethyl)thiazolidine (**amt**) units were achieved by two different synthetic pathways, both starting from the thiazolidine derivative **2** (Scheme 1). Thiazolidine **2** was obtained by condensation of *N*-Boc-glycine aldehyde[18] with L-cysteine methyl ester as a mixture of C-2 epimers (75% yield), which could not be separated by column chromatography. Their respective ^1H and ^{13}C resonances were assigned by 2D NMR experiments performed on the mixture. The two compounds were found to be present in a 65:35 ratio. A nuclear Overhauser effect between protons 2-H and 4-H was observed only in the case of the less abundant diastereomer, indicating that this corresponds to the *syn*-substituted thiazolidine. When the condensation was performed under different conditions (in the presence of triethylamine in dichloromethane containing $MgSO_4$), a 10:90 ratio of *anti*/*syn* diastereomers was found in the crude mixture. However, the 65:35 ratio was recovered after flash chromatographic purification of the crude mixture. These observations suggest that the *syn* diastereomer is the kinetic product. The 65:35 ratio of *anti*/*syn* diastereomers corresponds to the thermodynamic equilibrium state, the two diastereomers being in equilibrium through a ring-opened intermediate.[19] In an attempt to increase the proportion of the *anti* diastereomer, di-Boc-glycine aldehyde was substituted for Boc-glycine aldehyde in the thiazolidine condensation. This modification was expected to destabilize the *syn* diastereomer by introducing steric interactions between the C-2 and C-4 substituents or by preventing the formation of a hydrogen bond between these substituents. However, no significant change of the equilibrium ratio was observed.

The use of a highly reactive and nonhindered electrophile was necessary in order to obtain an *N*-acylated thiazolidine derivative featuring an *anti* relationship between the C-2 and C-4 substituents (vide infra). The *anti*-amtPNA monomer was prepared using the synthetic strategy outlined in Scheme 1. The mixture of thiazolidine **2** diastereomers was treated with chloroacetyl chloride in dichloromethane in the presence of pyridine at −78 °C to give a mixture of the *syn*- and *anti*-acylated products. These were separated by flash chromatography and found to be present in a 60:40 ratio (88% global yield). The more abundant product, **3a**, was crystallized, and X-ray analysis revealed an *anti* relationship between its C-2 and C-4 substituents (Figure 2). The NMR spectrum of compound **3a** showed the presence of the *cis* and *trans* isomers (about the amide bond) in equal proportions. In contrast, the existence of a major amide bond isomer (> 90%) was observed in the NMR spectrum of the *syn* compound **3b**. The conformation of the amide bond in the major and minor isomers could not be determined by NOESY experiments because of exchange-mediated magnetization transfer. In the next step, thymine was alkylated with **3a** and **3b** separately, in the presence of K_2CO_3 in anhydrous DMF, to give compounds **4a** and **4b**, respectively. The hydrolysis of the methyl ester was achieved by treatment with LiOH in dioxane/H_2O. After neutralization with $KHSO_4$, the Boc-protected amtPNA monomers **Boc-amt-T$_{anti}$** and **Boc-amt-T$_{syn}$** were obtained. No isomerization at the C-2 chiral centre during the last two steps was observed. The *anti*-**amt** monomer was isolated by precipitation from methanol (50% yield from **3a**) whereas the *syn* monomer needed a further flash chromatographic purification step (54% yield from **3b**). The NMR-spectroscopic data showed a 70:30 ratio of the two amide bond isomers for **Boc-amt-T$_{anti}$** and a 50:50 ratio for **Boc-amt-T$_{syn}$**.

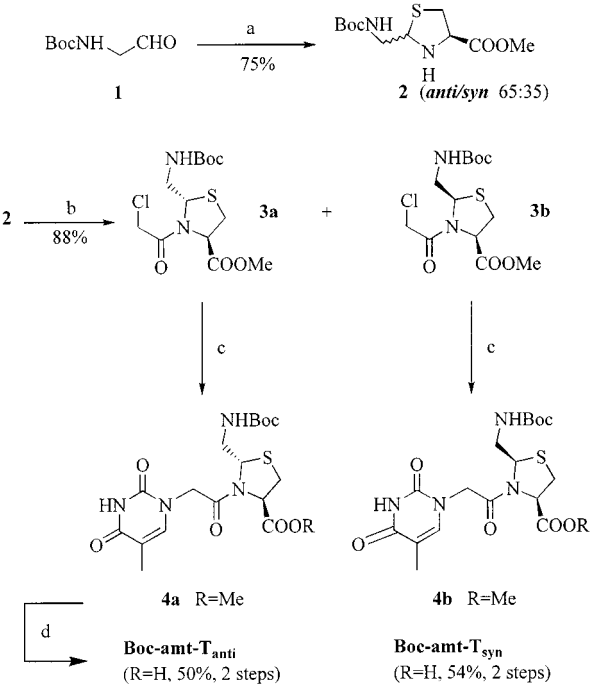

Scheme 1. a) Cys-OMe, pyridine, MeOH; b) $ClCH_2COCl$, pyridine, CH_2Cl_2, −78 °C; c) thymine, K_2CO_3, DMF; d) LiOH, H_2O/dioxane, then $KHSO_4$

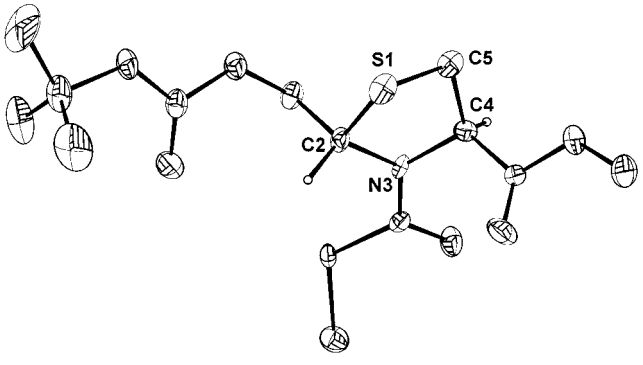

Figure 2. Cameron view[31] of one of the two crystallographically inequivalent molecules of **3a**

The *syn* compound **4b** was also obtained directly by treatment of thionyl chloride activated (1-thyminyl)acetic acid with the mixture of thiazolidine **2** diastereomers

(Scheme 2). Only the *syn*-acylated product was formed (78% yield), showing that the *syn*-thiazolidine **2** has a more favourable conformation for acylation by a hindered electrophile than the *anti*-thiazolidine **2** does. Compound **4b** was treated as described in Scheme 1 to give **Boc-amt-T$_{syn}$**.

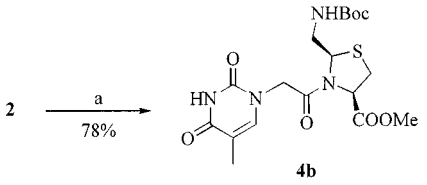

Scheme 2. a) (1-thyminyl)acetic acid, NaH, $SOCl_2$, DMF (−78 °C)

The abasic *syn*- and *anti*-**amt** monomers were also synthesized (Scheme 3). Compounds **5a** and **5b** were prepared by acetylation of a mixture of thiazolidine **2** diastereomers with acetyl chloride in the presence of pyridine at −78 °C. The two diastereomers were separated by flash chromatography and obtained in a 65:35 ratio (88% global yield). To investigate their respective stereochemistries, the Boc protecting groups were removed and the products treated with triethylamine (Scheme 3). Intramolecular cyclisation occurred only in the case of the less abundant product **5b**, to which *syn* stereochemistry, the only one that allows cyclisation, was assigned. Hydrolysis of **5b** gave the abasic **amt** monomer **Boc-amt-Ab$_{syn}$** (94%). Remarkably, during hydrolysis of the *anti* compound **5a**, isomerization at the C-2 chiral centre occurred. Hence, the expected product **Boc-amt-Ab$_{anti}$** was obtained in an equal proportion with a second compound, which was identified as **Boc-amt-Ab$_{syn}$** by its NMR-spectroscopic data and comparison of α_D values. The two diastereomers were separated by flash chromatography (67% global yield).

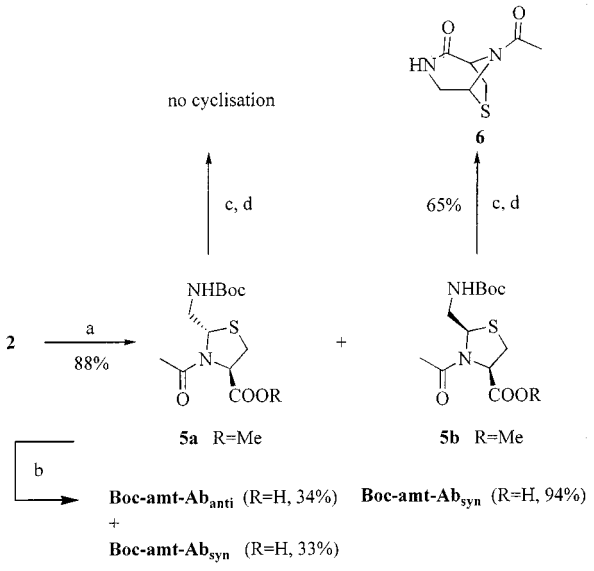

Scheme 3. a) CH_3COCl, pyridine, CH_2Cl_2, −78 °C; b) LiOH, H_2O/dioxane, then $KHSO_4$; c) TFA, CH_2Cl_2; d) Et_3N, CH_2Cl_2

PNA Solid-Phase Synthesis

To investigate the effect of the backbone constraint induced by the **amt** units on the stabilities of the PNA/DNA and PNA/RNA hybrids, a single modified unit was introduced into a central position of a 10-mer homothymine aegPNA (Table 1). Lysine was introduced at the C-terminus of the PNAs to reduce their self-aggregation after cleavage from resin.[20] PNAs were assembled manually on solid support. We applied, with minor modifications, the in situ neutralization protocol described by Schnölzer et al.[21] for Boc chemistry solid-phase peptide synthesis and used by Baird et al.[22] for the polymerization of DNA minor groove binding polyamides. Each coupling cycle consisted of: (1) treatment with TFA/*m*-cresol (95:5, v/v) to remove the Boc protecting group of the previously coupled monomer; (2) rapid flow wash with *N*-methylpyrrolidone (NMP); (3) simultaneous deprotonation of the terminal amino group of the polymer undergoing elongation and coupling of the next preactivated Boc-protected monomer (using high monomer concentration); (4) resin wash with NMP. A similar protocol has been applied by Christensen et al. to improve PNA polymerization by minimization of the *N*-acyl transfer side-reaction.[23] In a first series of experiments, we compared **aeg-T** unit coupling efficiencies when PNA assembly was performed on MBHA-PS or BHA-PEG-PS supports with similar low loading. In both cases we followed the coupling cycle described, and monomer activation was performed with HBTU/DIEA in NMP. Higher coupling yields were obtained with the MBHA-PS resin (97.5% HPLC average coupling yield, compared with 95% for the PEG-PS resin). Similar coupling efficiencies were observed when HBTU was replaced by HATU for assembly on PEG-PS support. In our hands, the introduction of a pyridine wash after Boc removal in the coupling cycle described above (as per Christensen et al.)[23] slightly reduced the coupling yield. MBHA-PS and active esters formed from HBTU/DIEA were used for the synthesis of the PNAs. The modified units were activated in the same way. Cleavage of the PNAs from the solid support was accomplished by the standard HF procedure. PNAs were purified by reverse phase HPLC and characterized by MALDI-TOF mass spectrometry. HPLC analyses of crude PNAs showed that the **amt** monomers had been incorporated efficiently. However, a drop in the coupling efficiency was observed for the incorporation of the *N*-terminal **aeg-T** unit during the assembly of **PNA-T$_{anti}$** and **PNA-Ab$_{anti}$**, which contain the *anti*-**amt** units. This was not observed in the synthesis of the PNAs containing the *syn*-**amt** units.

Thermal Stabilities of PNA/DNA and PNA/RNA Hybrids

Homopyrimidine aegPNAs are known to form PNA_2/DNA or PNA_2/RNA triplexes involving both Hoogsteen and Watson−Crick hydrogen bonding interactions; aegPNAs can bind to the DNA or RNA target in the parallel mode (N-terminus of the PNA facing the 5′-end of the target) or in the antiparallel mode (N/3′).[3] However, the triplex's stability is slightly increased when the

Table 1. Melting and half reassociation temperatures of the complexes[a]

DNA or RNA	**PNA-T_{anti}** X = amt-T_{anti}	**PNA-Ab_{anti}** X = amt-Ab_{anti}	**PNA-T_{syn}** X = amt-T_{syn}	**PNA-Ab_{syn}** X = amt-Ab_{syn}	**PNA_{ref}** X = aeg-T
$d(A_{10})$	55 (38.5)	45.5 (38.5)	50 (40.5)	50 (38.5)	72 (64)
$d(A_4TA_5)$	41.5 (26)	–	38 (29.5)	–	61.5 (45)
$d(A_5TA_4)$	41.5 (25.5)	–	36.5 (30)	–	62 (48)
poly(rA)	70.5 (68)	72 (67)	70 (68)	67 (63)	> 85

[a] Temperatures are given in °C. Half reassociation temperatures are indicated in brackets. PNAs sequence from N- to C-terminus: H−(aeg-T)$_4$−X−(aeg-T)$_5$−Lys−NH_2, X is specified in the table.

Watson−Crick PNA strand is in an antiparallel orientation relative to the oligonucleotide and the Hoogsteen PNA strand is in a parallel orientation.[24] The triplex formation is slow, which results in pronounced hystereses between the heating (triplex dissociation) and cooling (reassociation) UV absorbance curves.[3]

The stabilities of the modified PNA/DNA hybrids were estimated by UV melting experiments. Well-defined heating and cooling curves were obtained for all the modified hybrids, indicating that the presence of an **amt** unit in the centre of the PNA does not prevent the cooperative strands' dissociation and association. Significant hysteresis between the melting temperatures (T_m) and the half reassociation temperatures was observed, in agreement with the formation of PNA_2/DNA triplexes (Table 1). The UV melting experiments were performed using a 2:1 ratio of PNA/DNA.

When **PNA-T_{anti}** containing a single **amt-T_{anti}** unit was allowed to anneal to $d(A_{10})$ for 15 h at room temperature, a melting curve with a main sigmoid transition was obtained (Figure 3, **A**), as observed for the reference triplex **PNA_{ref}**/$d(A_{10})$ and indicating a simultaneous dissociation of both PNA strands from DNA. The T_m value for the modified triplex was found to be 55 °C, corresponding to a 17 °C decrease with respect to the T_m of the reference triplex (Table 1). When the annealing period was shorter (1 h), the melting curve for the modified triplex exhibited a double transition (Figure 3, **B**) whereas a single transition was still observed for the reference. The corresponding first derivative curve gave two peaks of comparable areas, with maxima at 40 °C and 55 °C (Figure 3, **B**). When the experiment was repeated with increasingly long annealing periods, the first peak (40 °C) progressively disappeared. The same observation was made when the PNA/DNA ratio was increased while the annealing period was kept constant (2 h) (data not shown). The results obtained with the modified PNA, together with the observation of particularly pronounced hysteresis (ΔT = 16.5 °C), suggest very slow triplex formation relative to duplex formation, the 40 and 55 °C peaks corresponding to the duplex and triplex melting temperatures, respectively. The presence of the **amt-T_{syn}** unit in the PNA (**PNA-T_{syn}**) also significantly reduced the thermal stability of the triplex formed with $d(A_{10})$ (22 °C decrease in T_m compared to the reference, Table 1). In this case, however, a single transition in the melting curve was observed after 1 h annealing time (Figure 3) while the hysteresis was close to that measured for the reference triplex (ΔT = 9.5 °C), suggesting that the **amt-T_{syn}** unit does not significantly affect the relative rate of triplex/duplex association.

Two sets of experiments were performed in order to test the stability and selectivity of the **amt** units base pairing. The hybridization of the PNAs containing the abasic **amt** units with $d(A_{10})$ was examined, and a thymine was introduced into the DNA strand opposite to the **amt-T** units. As the presence of the chiral **amt** unit in the PNA can influence its binding orientation to DNA, two mismatched DNA sequences, $d(A_4TA_5)$ and $d(A_5TA_4)$, were used to test both Hoogsteen and Watson−Crick **amt-T** units base pairing. In the case of the *anti*-**amt** unit, the removal of the nucleobase induced a 9.5 °C decrease in the T_m [Table 1, comparison of **PNA-Ab_{anti}**/$d(A_{10})$ and **PNA-T_{anti}**/$d(A_{10})$] suggesting that the **amt-T_{anti}** unit binds more strongly to the opposite adenine than the corresponding abasic unit. The observed triplex destabilization might be due to the loss of both hydrogen bonding and stacking interactions. Hybridization of **PNA-T_{anti}** to either mismatched DNA sequences resulted in a 13.5 °C decrease in the T_m, relative to the T_m of the **PNA-T_{anti}**/$d(A_{10})$ triplex (Table 1). An analogous effect was observed with **PNA_{ref}**, showing that base pairing selectivities are similar for the **amt-T_{anti}** unit and the nonmodified **aeg-T** unit. In the case of the *syn*-**amt** unit, the removal of the nucleobase had no effect on the triplex thermal stability [Table 1, comparison of **PNA-Ab_{syn}**/$d(A_{10})$ and **PNA-T_{syn}**/$d(A_{10})$]. In contrast, hybridization of **PNA-T_{syn}** to $d(A_4TA_5)$ and $d(A_5TA_4)$ caused reductions in the T_m, relative to hybridization to $d(A_{10})$, of 12 and 13.5 °C, respectively. One possible interpretation of the data obtained with the base removal experiment is that the nucleobase of the **amt-T_{syn}** unit is not hybridized to the opposite adenine and has no stacking interactions with the adjacent nucleobases. Steric hindrance, rather than hydrogen bonding loss, could be responsible for the destabilization observed when mismatch opposite to the modified unit is introduced.

As can be seen in Table 1, the hysteresis between the melting and the half reassociation temperatures depends on the PNA sequence. As mentioned before, this shows the different influences of the **amt** units on the kinetics of PNA association. The half reassociation temperature (T_{as}) reflects a phenomenon that discards more strongly from the thermodynamic equilibrium than the T_m, and so comparison of the complex stabilities on the basis of the T_{as} analysis is difficult.

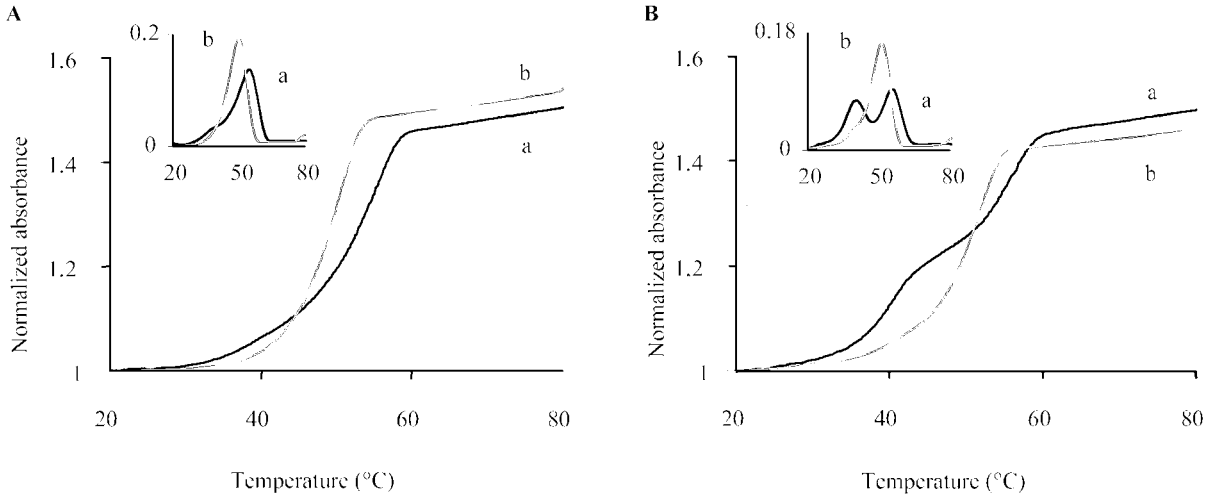

Figure 3. Melting curves and corresponding first derivative curves (insets) for the PNA-T_{anti}/d(A_{10}) complex (a) and the PNA-T_{syn}/d(A_{10}) complex (b); a 2:1 ratio of PNA/DNA was used; **A**: 15 h annealing time at room temperature; **B**: 1 h annealing time at room temperature

Binding of the modified PNA with poly(rA) was also tested. **PNA_{ref}** forms a very stable complex with poly(rA): hypochromicity was observed on mixing the PNA with the RNA, but no dissociation was observed when the sample was heated to 90 °C ($T_m > 85$ °C). The complexes formed with **PNA-T_{anti}** and **PNA-T_{syn}** exhibited lower thermal stabilities ($T_m = 70-71$ °C) (Table 1). The removal of the nucleobase of the *anti*-**amt** unit had no effect on the complex stability, suggesting that there is no base pairing of the modified unit. Hybridization of **PNA-Ab_{syn}** to poly(rA) induced a 3 °C decrease in the T_m relative to that of the **PNA-T_{syn}**/poly(rA) complex, suggesting that the base pairing of the **amt-T_{syn}** unit in the PNA/RNA complex is not efficient.

Molecular Recognition

Examination of the 3D structures of the complexes involving aegPNAs,[25] supplemented with molecular dynamics simulation studies,[26] have demonstrated the high flexibility of the aegPNA backbone. Six conformational states for the aegPNA backbone in the different types of complexes (PNA/DNA, PNA_2/DNA or PNA/RNA) have been characterized.[12] Three sets of values are observed for the (β, γ, δ) backbone torsion angles (Figure 1): (g^+, g^+, g^+), (t, g^-, g^+) and (g^-, g^-, g^-) (Table 2). The presence of the thiazolidine ring in the **amt** units restrains the backbone dihedral angles γ and δ (Figure 1). The fluctuation domains of the backbone torsion angle β and the side chain torsion angle χ_2 are also limited, due to steric interactions between

Table 2. Comparison of the sets of (β, γ, δ) backbone torsion angles values observed in the different aegPNA complexes[12] and in the **amt** units

	Range of torsion angles [°]/Rotamers						
	β			γ		δ	
aegPNA in:	80±20	180±30	−100±30	90±30	−100±30	80±30	−90±30
PNA_2/DNA PNA/DNA PNA/RNA	g^+			g^+		g^+	
PNA/DNA		t			g^-	g^+	
PNA/DNA			g^-		g^-		g^-
anti-**amt** unit	60±20 g^+	180±30 t		120±30 g^+ g^+		120±30 g^+ g^+	
syn-**amt** unit	60±20 g^+	180±30 t			−120±30 g^- g^-	120±30 g^+ g^+	

methylenes CD and CF (Figure 1). Each **amt** unit gives two possible sets for the β, γ and δ dihedral angles (Table 2). The *anti* **amt** unit is able to mimic the (g^+, g^+, g^+) rotamer observed in all different types of complexes mentioned above (Table 2). In contrast, the *syn*-**amt** unit is able to mimic the (t, g^-, g^+) rotamer, which is observed only in the PNA/DNA duplex (Table 2). Contradicting the expected effect, the experimental data show that the presence of an *anti*-**amt** unit in the PNA induces a significant destabilization of the PNA/DNA or PNA/RNA triplexes. No information about the effect of the *syn*-**amt** unit on the PNA/DNA duplex stability has been obtained in this study, but destabilization of the triplex has been observed. Surprisingly, similar PNA/DNA or PNA/RNA triplex stabilities are observed when the *syn*-and the *anti*-**amt** units are incorporated in the PNA.

The global destabilization of the modified complexes could be due to two effects: a local effect corresponding to the **amt-T** units' base pairing, and long-range effects corresponding to the adjacent **aeg-T** units' base pairing. The experimental data suggest that in the PNA/DNA triplex, base pairing occurs for the **amt-T_{anti}** unit but not for the **amt-T_{syn}** unit. However, the base pairing of the flanking **aeg-T** units seems to be more disturbed when the *anti*-**amt** unit is present, as suggested by the slightly lower thermal stability of the **PNA-Ab_{anti}**/d(A_{10}) triplex in comparison with that of the **PNA-Ab_{syn}**/d(A_{10}) triplex (Table 1). This study highlights the fact that restriction of the β, γ, and δ torsion angles is not sufficient to control correct pre-organisation of the PNA; the backbone topology must also be taken into account for any further modifications.

Conclusion

In this study we have presented the synthesis of two novel constrained PNA units. We have shown that their incorporation in a central position of the PNA strongly reduces the thermal stability of the PNA/DNA and PNA/RNA triplexes. Work using PNAs containing both purine and pyrimidine nucleobases to evaluate the effect of the **amt** units on PNA/DNA duplex stability and also on the PNA binding mode (parallel or antiparallel) to oligonucleotides is in progress.

Experimental Section

General Remarks: Standard reagents were of commercial quality (Acros, Aldrich, Merck, Senn Chemicals, SDS), *O*-(benzotriazol-1-yl)-1,1,3,3-tetramethyluronium hexafluorophosphate (HBTU) (Senn Chemicals), *O*-(7-azabenzotriazolyl)-1,1,3,3-tetramethyluronium hexafluorophosphate (HATU) (Millipore), benzhydrylamine polyethylene glycol polystyrene support (BHA-PEG-PS), 0.145 mmol/g (Millipore), 4-methylbenzhydrylamine polystyrene support (MBHA-PS), 0.9 mmol/g (Senn Chemicals). Oligonucleotides were purchased from Genset France. − Flash chromatography: Silica gel 60 (40−60 μm) (Merck). − Thin layer chromatography: Silica gel 60 F_{254} (Merck). − ^{1}H, ^{13}C NMR: DRX400, DRX500 instruments (Bruker). − NMR chemical shifts (δ) are given in ppm relative to solvent peak (^{1}H NMR: $CHCl_3$, δ = 7.27; CH_3OH, δ = 3.31; DMSO, δ = 2.50. − ^{13}C NMR: $^{13}CDCl_3$, δ = 77.23; $^{13}CD_3OD$, δ = 49.15; [D_6]DMSO, δ = 39.51). − Numbering of the thiazolidines is used to describe the NMR spectra. − CI mass spectra were performed using a triple quadrupole tandem mass spectrometer (R-30-10 Nemag). − MALDI-TOF mass spectrometry: Voyager Elite (PerSeptive Biosystems). − Microanalyses were performed by the "Service de Microanalyse de l'Université P. et M. Curie". Some of the compounds synthesized were found to be hygroscopic and no correct elemental analyses could be obtained. − UV melting curves were recorded using a UV/Vis spectrometer (Lambda 40, Perkin−Elmer) with a Peltier temperature programmer (PTP-6 Perkin−Elmer). − Other abbreviations used: diisopropylethylamine (DIEA), *N*,*N*-dimethylformamide (DMF), *N*-methylpyrrolidone-2 (NMP), T (thymine), trifluoroacetic acid (TFA).

Thiazolidine (2): L-Cysteine methyl ester hydrochloride (11.19 g, 65 mmol) was dissolved in methanol, and then pyridine (7.16 mL, 89 mmol) was added. This solution was quickly added to aldehyde **1** (9.42 g, 59 mmol) and the reaction mixture was stirred at room temperature overnight. The solution was concentrated under reduced pressure; the resulting residue was dissolved in CH_2Cl_2 and washed consecutively with a 10% aqueous $NaHCO_3$ solution and brine. The organic layer was dried with $MgSO_4$, filtered and concentrated to dryness. The residue was purified by flash chromatography on silica gel (EtOAc/cyclohexane, 4:6) to give the mixture of diastereomers **2** (12.2 g, 75%) as a colourless, viscous oil. − R_f = 0.5 (EtOAc/cyclohexane, 1:1). − ^{1}H NMR (400 MHz, $CDCl_3$, mixture of 2 diastereomers *anti*/*syn* 65:35): δ = 5.22 (m, 1 H, Boc-N*H*, *anti*), 5.12 (m, 1 H, Boc-N*H*, *syn*), 4.72 (dd, *J* = 8.2, 5.1 Hz, 1 H, 2-H *anti*), 4.60 (dd, *J* = 5.0 Hz, 1 H, 2-H, *syn*), 3.90 (dd, *J* = 7.6, 6.5 Hz, 1 H, 4-H, *anti*), 3.81 (dd, *J* = 9.2, 6.5 Hz, 1 H, 4-H, *syn*), 3.71 (s, 6 H, OCH_3), 3.19−2.79 (m, 8 H, 5-H, $HNCH_2$), 1.37, 1.36 (2 s, 18 H, CH_3 Boc). − ^{13}C NMR (62.9 MHz, $CDCl_3$, mixture of diastereomers): δ = 171.6, 171.4, 155.9, 155.7 (CO), 69.5 (C-2, *syn*), 68.2 (C-2, *anti*), 65.4 (C-4, *syn*), 63.3 (C-4, *anti*), 52.5 (OCH_3), 45.9 ($HNCH_2$, *anti*), 43.5 ($HNCH_2$, *syn*), 37.9 (C-5, *syn*), 37.7 (C-5, *anti*), 28.3 (CH_3 Boc). − CI-MS (NH_3): *m*/*z* = 277 $[M + H]^+$. − $C_{11}H_{20}N_2O_4S$ (276.35): calcd. C 47.80, H 7.294, N 10.13; found C 47.81, H 7.35, N 10.09.

Chloro Compounds 3a and 3b: Chloroacetyl chloride (5.1 mL, 37 mmol) was added dropwise over a period of 10 min to a mixture of **2** (8.66 g, 31 mmol) and pyridine (3.80 mL, 47 mmol) in CH_2Cl_2 at −78 °C, and the reaction mixture was stirred vigorously at this temperature. After 1 h, the mixture was diluted with dichloromethane and washed with 10% aqueous citric acid solution and brine. After drying with $MgSO_4$, the organic layer was filtered and concentrated. The resulting residue was purified by flash chromatography on silica gel. Elution with EtOAc/cyclohexane (3:7) permitted the isolation of compounds **3a** (5.83 g) and **3b** (3.89 g) (60:40 ratio of **3a**/**3b**, 88% global yield). Compound **3a** was crystallized from ethyl acetate, **3b** was obtained as yellow foam.

Compound 3a: R_f = 0.36 (EtOAc/cyclohexane, 1:1). − ^{1}H NMR (400 MHz, $CDCl_3$): (mixture of two amide bond isomers: 50:50) δ = 5.30 (m, 1 H, 2-H), 5.15 (m, 2 H, 2-H, Boc-N*H*), 4.94 (m, 2 H, 4-H, Boc-N*H*), 4.90 (d, *J* = 7.1 Hz, 1 H, 4-H), 4.42 (2 d, 2 H, *J* = 13.0 Hz, $ClCH_2$), 3.97 (2 d, 2 H, *J* = 13.0 Hz, $ClCH_2$), 3.79, 3.76 (2 s, 6 H, OCH_3), 3.61−2.90 (m, 8 H, 5-H, $HNCH_2$), 1.42 (s, 18 H, CH_3 Boc). − ^{13}C NMR (62.9 MHz, $CDCl_3$): δ = 170.1, 169.4, 166.5, 165.6, 155.94, 155.93 (CO), 64.7, 63.3 (C-2), 63.3, 63.1 (C-4), 53.6, 52.9 (OCH_3), 46.6, 44.2 ($HNCH_2$), 42.8, 41.5 ($ClCH_2$),

33.4, 30.7 (C-5), 28.3 (CH_3 Boc). − CI-MS (NH_3): *m/z* = 353 [M + H]$^+$. − $C_{13}H_{21}ClN_2O_5S$ (352.84): calcd. C 44.15, H 5.99, N 7.94; found C 44.43, H 6.03, N 7.81. − $[\alpha]_D^{20}$ = −142 (*c* = 1, CH_2Cl_2).

Compound 3b: R_f = 0.50 (EtOAc/cyclohexane, 1:1). − ^{1}H NMR (400 MHz, $CDCl_3$): δ = 5.38 (m, 1 H, Boc-N*H*), 5.28 (t, *J* = 8.4 Hz, 1 H, 2-H), 5.00 (t, *J* = 8.4 Hz, 1 H, 4-H), 4.32, 4.14 (2 d, 2 H, *J* = 13.1 Hz, $ClCH_2$), 3.79 (s, 3 H, OCH_3), 3.56−3.10 (m, 4 H, 5-H, HNC*H*$_2$), 1.41 (s, 9 H, CH_3 Boc). − ^{13}C NMR (62.9 MHz, $CDCl_3$): δ = 171.6, 165.0, 156.0 (CO), 62.8 (C-2), 62.0 (C-4), 53.1 (OCH_3), 45.9 ($HNCH_2$), 41.4 ($ClCH_2$), 31.4 (C-5), 28.3 (CH_3 Boc). − CI-MS (NH_3): *m/z* = 353 [M + H]$^+$. − $C_{13}H_{21}ClN_2O_5S$ (352.84): calcd. C 44.15, H 5.99, N 7.94; found C 44.38, H 6.01, N 7.83. − $[\alpha]_D^{20}$ = −117 (*c* = 1, CH_2Cl_2).

Boc-amt-T$_{anti}$-methyl Ester (4a) and Boc-amt-T$_{syn}$-methyl Ester (4b): A mixture of thymine (2.03 g, 16.06 mmol), pulverized K_2CO_3 (9.25 g, 67 mmol) and **3a** (4.72 g, 13.4 mmol) in anhydrous DMF was stirred at room temperature for 5 h. K_2CO_3 was removed by filtration through Celite and DMF was evaporated under reduced pressure. The resulting residue was purified by flash chromatography on silica gel (EtOAc/cyclohexane, 9:1) to give **4a** (3.95 g, 67%) as an amorphous white solid. The same procedure was applied starting from **3b** (2.50 g, 7.09 mmol), thymine (1.07 g, 8.5 mmol) and K_2CO_3 (4.9 g, 35 mmol). Purification was performed by flash chromatography (EtOAc) to afford **4b** (2.20 g, 70%) as an amorphous, white solid. Access to **4b** according to Scheme 2: NaH (230 mg, 9.6 mmol) was added to (1-thyminyl)-acetic acid (1.6 g, 8.7 mmol) in DMF. The mixture was sonicated until complete formation of the sodium salt (15 min), cooled in an ice bath, and thionyl chloride (635μL, 8.7 mmol) was added dropwise. Agitation was maintained over 2 min at 0 °C, followed by sonication until a yellow solution was obtained. This solution was then cooled to −78 °C and thiazolidine **2** (2 g, 7.2 mmol), dissolved in DMF in the presence of pyridine (700 μL, 8.7 mmol), was added slowly. The mixture was stirred at room temperature for 1 h 30. DMF was removed by evaporation under reduced pressure and the resulting residue was dissolved in EtOAc. The organic layer was washed with an aqueous citric acid solution. After drying with $MgSO_4$, the solvent was removed under vacuum and the resulting residue was purified by flash chromatography on silica gel (EtOAc) to afford **4b** (2.5 g, 78%).

Compound 4a: R_f = 0.25 (EtOAc). − ^{1}H NMR (500 MHz, [D$_6$]DMSO) (mixture of two amide bond isomers, 60:40): δ = 7.38, 7.26 (2 s, 2 H, CH T), 7.29, 6.86 (2 m, 2 H, Boc-N*H*), 5.24 (m, 2 H, 2-H maj., 4-H min.), 5.13 (dd, *J* = 7.3, 2.9 Hz, 1 H, 2-H min.), 4.79 (s, 2 H, T-CH_2 maj.), 4.67 (d, *J* = 7.7 Hz, 1 H, 4-H maj.), 4.56, 4.34 (2 d, 2 H, *J* = 16.8 Hz, T-CH_2 min.), 3.74, 3.60 (2 s, 6 H, OCH_3), 3.55−3.10 (m, 8 H, 5-H, HNC*H*$_2$), 1.76, 1.75 (2 s, 6 H, CH_3 T), 1.38 (s, 18 H, CH_3 Boc). − ^{13}C NMR (125.7 MHz, [D$_6$]DMSO): δ = 170.3, 169.3, 166.5, 165.2, 164.33, 164.30, 155.9, 155.7 (CO), 141.9, 141.7 (CH T), 108.3, 108.2 (H_3C-*C* T), 64.1 (C-2), 62.2 (C-2), 62.2 (C-4), 61.9 (C-4), 53.1, 52.0 (OCH_3), 49.1, 48.5 (T-CH_2), 45.0, 43.0 ($HNCH_2$), 32.7, 30.2 (C-5), 28.2, 28.1 (CH_3 Boc), 11.9 (CH_3 T). − CI-MS (NH_3): *m/z* = 443 [M + H]$^+$. − $C_{18}H_{26}N_4O_7S$ (442.49): calcd. C 48.85, H 5.92, N 12.66; found C 48.69, H 5.95, N 12.51. − $[\alpha]_D^{20}$ = −105 (*c* = 1, DMF).

Compound 4b: R_f = 0.35 (EtOAc). − ^{1}H NMR (400 MHz, $CDCl_3$): δ = 9.67 (s, 1 H, NH T), 6.97 (s, 1 H, CH T), 5.59 (m, 1 H, Boc-N*H*), 5.30 (t, *J* = 7.1 Hz, 1 H, 2-H), 4.94 (t, *J* = 8.6 Hz, 1 H, 4-H), 4.89, 4.35 (2 d, 2 H, *J* = 16.0 Hz, T-CH_2), 3.73 (s, 3 H, OCH_3), 3.60−3.10 (m, 4 H, 5-H and HNC*H*$_2$), 1.86 (s, 3 H, CH_3 T), 1.40 (s, 9 H, CH_3 Boc). − ^{13}C NMR (62.9 MHz, $CDCl_3$): δ = 171.4, 165.1, 164.4, 156.0, 151.1 (CO), 140.8 (CH T), 110.7 (H_3C-*C* T), 62.5 (C-2), 62.3 (C-4), 53.0 (OCH_3), 48.7 (T-CH_2), 47.8 ($HNCH_2$), 33.0 (C-5), 28.3 (CH_3 Boc), 12.3 (CH_3 T). − CI-MS (NH_3): *m/z* = 443 [M + H]$^+$. − $[\alpha]_D^{20}$ = −135 (*c* = 1.5, CH_2Cl_2).

PNA Monomers (Boc-amt-T$_{anti}$ and Boc-amt-T$_{syn}$): LiOH hydrate (631 mg, 15.05 mmol) was added in portions to a solution of **4a** (5.55 g, 12.54 mmol) in dioxane/H_2O (3:2) (20 mL). The reaction mixture was stirred at room temperature until all the starting material had been consumed. The dioxane was evaporated and water was added. The aqueous layer was washed twice with CH_2Cl_2, neutralized with $KHSO_4$ (2.05 g, 15.05 mmol) and concentrated under vacuum. The resulting residue was triturated with MeOH and the sulfate salts were removed by filtration. The filtrate was concentrated to a small volume and left at −10 °C overnight to allow precipitation. The solid was filtered, and washed with ethanol and ether to afford **Boc-amt-T$_{anti}$** (4.03 g, 75%) as a white solid. The same procedure was applied starting from **4b** (1.2 g, 2.7 mmol) and LiOH hydrate (136 mg, 3.25 mmol). After neutralization with $KHSO_4$ (442 mg, 3.25 mmol) and filtration of the sulfate salts, no precipitation had occurred, even at low temperature. Purification was performed by flash chromatography on silica gel (CH_2Cl_2/MeOH/AcOH, 85:15:0.5) to afford **Boc-amt-T$_{syn}$** (890 mg, 77%) as an amorphous white solid.

Boc-amt-T$_{anti}$: ^{1}H NMR (400 MHz, [D$_6$]DMSO): δ = 11.35, 11.30 (2 s, 1 H, NH T), 7.38, 7.29 (2 s, 1 H, CH T), 6.86, 6.52 (2 m, 1 H, Boc-N*H*), 5.17 (dd, 0.3 H, *J* = 8.6, 3.6 Hz, 2-H), 5.32 (dd, 0.7 H, *J* = 7.6, 3.6 Hz, 2-H), 4.96 (t, 0.7 H, 4-H), 4.22−4.91 (m, 2.3 H, 4-H, T-C*H*$_2$), 3.01−3.55 (m, 4 H, 5-H, HNC*H*$_2$), 1.75, 1.74 (2 s, 3 H, CH_3 T), 1.37 (2 s, 9 H, CH_3 Boc). − ^{13}C NMR (62.9 MHz, [D$_6$]DMSO): δ = 171.4, 170.3, 166.8, 165.2, 164.4, 155.9, 155.7 (CO), 142.2, 141.8 (CH T), 108.3, 108.2 (H_3C-*C* T), 78.3, 77.8 (C_q Boc), 64.0 (C-2), 62.9 (C-4), 62.4 (C-4), 62.1 (C-2), 49.1, 48.7 (T-CH_2), 45.2, 43.2 ($HNCH_2$), 33.0, 30.4 (C-5), 28.2 (CH_3 Boc), 11.9 (CH_3 T). − $[\alpha]_D^{20}$ = −95 (*c* = 1, DMF).

Boc-amt-T$_{syn}$: ^{1}H NMR (400 MHz, [D$_6$]DMSO): δ = 11.35, 11.31 (2 s, 1 H, NH T), 7.41, 7.33 (2 s, 1 H, CH T), 7.07, 6.87 (2 m, 1 H, Boc-N*H*), 5.38 (dd, 0.5 H, *J* = 7.6, 5.1 Hz, 2-H), 5.32 (dd, 0.5 H, *J* = 8.6, 5.1 Hz, 2-H), 4.30−4.90 (m, 3 H, 4-H, T-C*H*$_2$), 3.04−3.48 (m, 4 H, 5-H, HNC*H*$_2$), 1.74, 1.73 (2 s, 3 H, CH_3 T), 1.37, 1.34 (2 s, 9 H, CH_3 Boc). − ^{13}C NMR (62.9 MHz, [D$_6$]DMSO): δ = 173.0, 172.2, 165.7, 165.1, 164.6, 155.9, 155.7 (CO), 142.2, 142.2 (CH T), 108.4, 108.3 (H_3C-*C* T), 78.5, 77.9 (C_q Boc), 63.6 (C-2), 63.2 (C-4), 62.8 (C-4), 62.5 (C-2), 48.8, 48.4 (T-CH_2), 45.1, 43.5 ($HNCH_2$), 33.6, 31.0 (C-5), 28.32, 28.28 (CH_3 Boc), 12.1 (CH_3 T). − $[\alpha]_D^{20}$ = −78 (*c* = 0.75, MeOH).

Boc-amt-Ab$_{anti}$-methyl Ester (5a) and Boc-amt-Ab$_{syn}$-methyl Ester (5b): Acetyl chloride (1.7 mL, 24 mmol) was added dropwise over a period of 10 min to a mixture of **2** (5.55 g, 20 mmol) and pyridine (2.43 mL, 30 mmol) in CH_2Cl_2 at −78 °C. The reaction mixture was stirred vigorously for 30 min at this temperature. Dichloromethane was added and the organic layer was washed with a 10% aqueous citric acid solution and brine. After drying with $MgSO_4$, the organic phase was filtered and concentrated. The resulting residue was purified by flash chromatography on silica gel. Elution with EtOAc/cyclohexane (4:6) permitted the isolation of compounds **5a** (3.37 g) and **5b** (1.81 g) (65:35 ratio of **5a**/**5b**, 76% global yield).

Compound 5a: R_f = 0.20 (EtOAc/cyclohexane, 7:3). − ^{1}H NMR (400 MHz, $CDCl_3$) (mixture of two amide bond isomers 60:40): δ = 5.25 (m, 2 H, 2-H min., Boc-N*H* maj.), 5.12 (s, 1 H, Boc-N*H* min.), 5.06 (dd, *J* = 9.1, 4.0 Hz, 1 H, 2-H maj.), 4.80 (d, *J* =

7.2 Hz, 1 H, 4-H maj.), 4.69 (d, J = 6.1 Hz, 1 H, 4-H min.), 3.73, 3.67 (2 s, 6 H, OCH_3), 3.62−2.89 (m, 8 H, 5-H, HNCH_2), 2.28, 1.97 (2 s, 6 H, CH_3 Ac), 1.37 (s, 18 H, CH_3 Boc). − ^{13}C NMR (62.9 MHz, $CDCl_3$): δ = 170.3, 170.1, 169.9, 169.5, 155.9, 155.8 (CO), 64.1, 64.1 (C-2), 64.1, 62.4 (C-4), 53.1, 52.5 (OCH_3), 45.6, 44.7 ($HNCH_2$), 33.4, 30.9 (C-5), 28.2 (CH_3 Boc), 23.5, 22.2 (CH_3 Ac). − CI-MS (NH_3): m/z = 319 [M + H]$^+$. − $C_{13}H_{22}N_2O_5S$ (318.39): calcd. C 49.04, H 6.96, N 8.80; found C 49.19, H 7.21, N 8.69. − $[\alpha]_D^{20}$ = −86 (c = 1, CH_2Cl_2).

Compound 5b: R_f = 0.40 (EtOAc/cyclohexane, 7:3). − ^{1}H NMR (400 MHz, $CDCl_3$): δ = 5.45 (m, 1 H, Boc-N*H*), 5.04 (t, J = 7.1 Hz, 1 H, 2-H), 4.80 (t, J = 8.2 Hz, 1 H, 4-H), 3.59 (s, 3 H, OCH_3), 3.35−2.99 (m, 4 H, 5-H, HNCH_2), 2.04 (s, 3 H, CH_3 Ac), 1.26 (s, 9 H, CH_3 Boc). − ^{13}C NMR (62.9 MHz, $CDCl_3$): δ = 170.7, 168.6, 155.6 (CO), 63.2 (C-2), 61.0 (C-4), 53.0 (OCH_3), 45.2 ($HNCH_2$), 31.2 (C-5), 28.0 (CH_3 Boc), 21.5 (CH_3 Ac). − CI-MS (NH_3): m/z = 319 [M + H]$^+$. − $C_{13}H_{22}N_2O_5S$: calcd. C 49.04, H 6.96, N 8.80; found C 49.05, H 7.23, N 8.62. − $[\alpha]_D^{20}$ = −141 (c = 0.75, CH_2Cl_2).

Abasic PNA Monomers (Boc-amt-Ab$_{anti}$ and Boc-amt-Ab$_{syn}$): LiOH hydrate (16.3 mg, 389 μmol) was added in portions to a solution of **5b** (103 mg, 324 μmol) in dioxane/H_2O (3:2) (1 mL). The suspension was stirred at room temperature until all the starting material was consumed, the dioxane was then evaporated and water was added. The aqueous layer was washed twice with CH_2Cl_2, neutralized with $KHSO_4$ (52 mg, 389 μmol) and concentrated. The resulting residue was triturated with MeOH, the sulfate salts were filtered and the filtrate was concentrated under reduced pressure to give pure **Boc-amt-Ab$_{syn}$** (92 mg, 94%) as an amorphous solid. The same procedure was applied to compound **5a** (253 mg, 795 μmol), using LiOH hydrate (40 mg, 954 μmol) and $KHSO_4$ (130 mg, 954 μmol), to give a mixture of **Boc-amt-Ab$_{anti}$** and **Boc-amt-Ab$_{syn}$**, which were separated by flash chromatography on silica gel. Elution with CH_2Cl_2/MeOH (9:1) gave **Boc-amt-Ab$_{anti}$** (82 mg) and **Boc-amt-Ab$_{syn}$** (80 mg) (67% total yield).

Boc-amt-Ab$_{anti}$: ^{1}H NMR (400 MHz, CD_3OD) (mixture of two amide bond isomers 70:30): δ = 5.28 (dd, J = 3.3, 6.7 Hz, 1 H, 2-H maj.), 5.16 (dd, J = 7.9, 4.5 Hz, 1 H, 2-H min.), 4.68 (m, 2 H, 4-H min., 4-H maj.), 3.60−3.10 (m, 8 H, 5-H, HNCH_2), 2.33, 2.10 (2 s, 6 H, CH_3 Ac), 1.46, 1.45 (2 s, 18 H, CH_3 Boc). − ^{13}C NMR (62.9 MHz, CD_3OD): δ = 177.8, 173.9, 172.5, 159.1, 158.8 (CO), 68.1, 66.1 (C-4), 66.4, 66.1 (C-2), 47.1, 45.3 ($HNCH_2$), 35.2, 33.3 (C-5), 29.3 (CH_3 Boc), 24.5, 23.2 (CH_3 Ac). − CI-MS (NH_3): m/z = 305 [M + H]$^+$. − $[\alpha]_D^{20}$ = −91 (c = 0.75, MeOH).

Boc-amt-Ab$_{syn}$: ^{1}H NMR (400 MHz, CD_3OD) (mixture of two amide bond isomers 50:50): δ = 5.50 (t, J = 6.0 Hz, 1 H, 2-H), 5.27 (t, J = 7.0 Hz, 1 H, 2-H), 4.80 (t, J = 8.6 Hz, 1 H, 4-H), 4.68 (t, J = 7.3 Hz, 1 H, 4-H), 3.65−3.21 (m, 8 H, 5-H, HNCH_2), 2.24, 2.10 (2 s, 6 H, CH_3 Ac), 1.46, 1.45 (2 s, 18 H, CH_3 Boc). − ^{13}C NMR (62.9 MHz, CD_3OD): δ = 177.2, 176.6, 172.8, 171.8, 159.0, 158.7 (CO), 67.4, 65.8 (C-4), 65.5, 64.8 (C-2), 46.79, 45.76 ($HNCH_2$), 35.8, 33.5 (C-5), 29.2 (CH_3 Boc), 23.2, 22.7 (CH_3 Ac). − CI-MS (NH_3): m/z = 305 [M + H]$^+$. − $[\alpha]_D^{20}$ = −54 (c = 1, DMF).

Compound 6: Compound **5b** (235 mg, 739 μmol) was treated with a mixture of TFA and CH_2Cl_2 (1:1, 1 mL) for 10 min. The solution was concentrated, the resulting residue was dissolved in CH_2Cl_2 and Et_3N (0.5 mL) was added slowly. The mixture was stirred at room temperature for 24 h and concentrated to dryness, and the residue was purified by flash chromatography on silica gel (EtOAc) to give **6** (90 mg, 65%) as an amorphous solid. − ^{1}H NMR (400 MHz, $CDCl_3$) (mixture of two amide bond isomers 60:40): δ = 7.40, 7.21 (2 s, 2 H, NH), 6.07 (s, 1 H, 2-H maj.), 5.46 (s, 1 H, 2-H min.), 5.46 (d, J = 3.9 Hz, 1 H, 4-H min.), 5.76 (d, J = 5.1 Hz, 1 H, 4-H maj.), 3.90−3.05 (m, 8 H, 5-H, HNCH_2), 2.13, 2.07 (2 s, 6 H, CH_3 Ac). − ^{13}C NMR (62.9 MHz, $CDCl_3$): δ = 169.3, 168.7, 168.1, 167.1 (CO), 61.0, 57.7 (C-2), 57.5, 53.5 (C-4), 50.8, 49.9 ($HNCH_2$), 38.6, 37.6 (C-5), 21.5 (CH_3 Ac). − CI-MS (NH_3): m/z = 187 [M + H]$^+$. − $C_7H_{10}N_2O_2S$ (186.23): calcd. C 45.15, H 5.41, N 15.04; found C 45.39, H 5.55, N 14.81. − $[\alpha]_D^{20}$ = −81 (c = 1, CH_2Cl_2).

PNA Assembly: PNAs were synthesized manually on a 10-μmol scale. Typically, dry MBHA-PS resin (22.2 mg, 0.9 mmol NH_2/g) was placed in a fritted funnel and swollen overnight in CH_2Cl_2 (0.5 mL). It was washed successively with 10% triethylamine in CH_2Cl_2 (0.5 mL), CH_2Cl_2 (2 × 1 mL) and NMP (2 × 1 mL). It was treated with a limited amount of activated Boc-Lys-(Z-Cl-2) to achieve a loading of 0.45 mmol NH_2/g: the Boc-Lys-(Z-Cl-2) (5 mg, 0.012 mmol) was pre-activated for 1 min with HBTU (4 mg, 0.01 mmol) and DIEA (21 μL, 0.12 mmol) in NMP (200 μL final volume) and then added to the resin. Coupling was allowed to proceed for 30 min. Capping of unchanged amino groups was performed by acetylation with 1 mL 10% acetic anhydride in NMP. The resin was washed with NMP (30 s flow wash). For assembly of the PNA monomers, the following coupling cycle was used: (1) Boc removal: addition of 0.5 mL of TFA/*m*-cresol (95:5, v/v), stirring with argon bubbling for 30 s and draining, addition of 1 mL of TFA/*m*-cresol, stirring for 5 min and draining, NMP flow washing for 30 s, stirring with NMP for 20 s, draining carefully. (2) Preactivation of the Boc-protected monomer (0.25 M final concentration) for 2 min at 40 °C: 180 μL of a 0.25 M solution of HBTU in NMP (0.045 mmol, 4.5 equiv. based on the amount of resin) were added to the monomer (0.05 mmol, 5 equiv./resin) followed by addition of 21 μL of DIEA (0.12 mmol, 12 equiv./resin). (3) Addition of the activated monomer to the resin and stirring with argon bubbling for 15 min, draining and washing with NMP (20 s stirring, 20 s flow washing), draining. At the end of the synthesis, the resin was washed twice each with 2 mL NMP, 2 mL CH_2Cl_2 and 2 mL methanol and dried in vacuum. Cleavage from the resin was performed by treatment with HF with addition of anisole (1.5 mL/g of resin) and dimethyl sulfide (250 μL/g of resin) for 1 h at 0 °C. PNAs were purified by reversed-phase HPLC using an RP-8 column (5 μm) heated at 55 °C (monitoring at 220 nm). Separation was performed using a linear gradient of buffer B in A (20 to 45% B in A over 40 min at a flow rate of 1.5 mL/min) with buffer A = 0.1% aqueous TFA and buffer B = acetonitrile/buffer A (1:1). − PNAs were characterized by MALDI-TOF mass spectrometry in the positive-ion mode using α-cyano-4-hydroxycinnamic acid as matrix; m/z: **PNA-T$_{anti}$**: 2851.9 [M + H]$^+$ (calcd. 2851.9); **PNA-T$_{syn}$**: 2852.1 [M + H]$^+$ (calcd. 2851.9); **PNA-Ab$_{anti}$**: 2727.2 [M + H]$^+$ (calcd. 2727.8); **PNA-Ab$_{syn}$**: 2727.0 [M + H]$^+$ (calcd. 2727.8); **PNA$_{ref}$**: 2807.4 [M + H]$^+$ (calcd. 2807.8).

UV Melting Experiments: PNA concentrations were determined by measuring the absorbance at 260 nm of a sample heated at 80 °C, using a molar extinction coefficient at 260 nm for T = 8.8 $mM^{-1}cm^{-1}$. UV melting experiments were carried out in 10 mM sodium phosphate buffer (pH = 7) containing 100 mM NaCl and 0.1 mM EDTA. The PNA strand (4 μM) and DNA strand (2 μM) were mixed in the buffer, heated at 90 °C for 10 min, then cooled to room temperature and stored overnight at room temperature. If the starting temperature for T_m measurement was 10 °C, samples were stored at 10 °C for at least 30 min before starting the experiment. Samples were heated from 10 or 20 °C to 90° and cooled back to 10 or 20 °C at a rate of 0.5 °C/min.

X-ray Crystallographic Study of Compound 3a: Crystal data and data collection information are summarized in Table 3. Data were corrected for Lorentz and polarization effects. No absorption correction was applied. The structure was solved by direct methods using SHELXS,[27] all other calculations used CRYSTALS.[28] Atomic scattering factors and anomalous dispersion terms were taken from D. T. Cromer.[29] Full-matrix, least-squares refinement based on |F| and a Chebychev weighting scheme[30] were performed. All non-hydrogen atoms were anisotropically refined. Hydrogen atoms were introduced in calculated positions and were allocated one overall refinable isotropic thermal parameter. Crystallographic data (excluding structure factors) for the structure reported in this paper have been deposited with the Cambridge Crystallographic Data Centre as supplementary publication no. CCDC-158700. Copies of the data can be obtained free of charge on application to CCDC, 12 Union Road, Cambridge CB2 1EZ, UK [Fax: (internat.) + 44-1223/336-033; E-mail: deposit@ccdc.cam.ac.uk].

Table 3. Crystal data and data collection information for $C_{13}H_{21}ClN_2O_5S$

Molecular mass	352.8
Crystal size [mm]	0.4 × 0.4 × 0.6
a [Å]	6.897(4)
b [Å]	10.168(5)
c [Å]	13.740(6)
α [°]	93.01(4)
β [°]	104.67(4)
γ [°]	109.86(5)
V [Å^3]	866.5(9)
Z	2
Crystal system	triclinic
Space group	*P*1
Linear absorption coefficient μ [cm^{-1}]	3.55
ρ [g cm^{-3}]	1.35
Diffractometer	Enraf−Nonius MACH3
Radiation	Mo-K_α (λ = 0.71069 Å)
Scan type	ω/2θ
Scan range [°]	0.8 + 0.345 tgθ
θ limits [°]	1−25
Temperature [K]	295
Octants collected	*h*: 0, 8; *k*: −12, 11; *l*: −16, 15
No. of data collected	3308
No. of unique data collected	3031 (R_{int} = 0.01)
No. of unique data used for refinement	2150 $(F_o)^2 > 3\sigma(F_o)^2$
$R = \Sigma\|\|F_o\| - \|F_c\|\|/\Sigma\|F_o\|$	0.0773
Rw[a] = $[\Sigma w(\|F_o\| - \|F_c\|)^2/\Sigma wF_o^2]1/2$	0.0912
S	1.07
Extinction parameter	none
No. of variables	398
Δρmin [e·Å^{-3}]	−0.51
Δρmax [e·Å^{-3}]	0.70

[a] $w = w'\cdot[1-[(|F_o| - |F_c|)/6\cdot\sigma(F_o)]^2]^2$ with $w' = 1/\Sigma r\cdot A_r T_r(X)$ with 3 coefficients 5.56, 1.52 and 3.68 for a Chebyshev series, for which X is F_c/F_c(max).

Acknowledgments

We thank Dr. Gérard Bolbach for recording the MALDI-TOF mass spectra. We would also like to thank Dr. Anna Garbesi and Dr. Nicole Goasdoué for helpful discussions.

[1] P. E. Nielsen, M. Egholm, R. H. Berg, O. Buchardt, *Science* **1991**, *254*, 1497−1500.
[2] A. Ray, B. Nordén, *FASEB* **2000**, *14*, 1041−1060.
[3] For reviews, see: [3a] B. Hyrup, P. E. Nielsen, *Bioorg. Med. Chem.* **1996**, *4*, 5−23. − [3b] D. R. Corey, *TIBTECH* **1997**, *15*, 224−229. − [3c] E. Uhlmann, A. Peyman, G. Breipohl, D. W. Will, *Angew. Chem. Int. Ed.* **1998**, *37*, 2796−2823. − [3d] P. E. Nielsen, *Acc. Chem. Res.* **1999**, *32*, 624−630.
[4] K. N. Ganesh, P. E. Nielsen, *Curr. Org. Ohem.* **2000**, *4*, 931−943.
[5] P. Lagriffoule, P. Wittung, M. Eriksson, K. K. Jensen, B. Nordén, O. Buchardt, P. E. Nielsen, *Chem. Eur. J.* **1997**, *3*, 912−919.
[6] [6a] B. P. Gangamani, V. A. Kumar, K. N. Ganesh, *Tetrahedron* **1996**, *52*, 15017−15030. − [6b] B. P. Gangamani, V. A. Kumar, K. N. Ganesh, *Tetrahedron* **1999**, *55*, 177−192.
[7] [7a] S. Jordan, C. Schwemler, W. Kosch, A. Kretschmer, E. Schwenner, U. Stropp, B. Mielke, *Bioorg. Med. Chem. Lett.* **1997**, *7*, 681−686.[7b] S. Jordan, C. Schwemler, W. Kosch, A. Kretschmer, U. Stropp, E. Schwenner, B. Mielke, *Bioorg. Med. Chem. Lett.* **1997**, *7*, 687−690.
[8] [8a] M. D'Costa, V. A. Kumar, K. N. Ganesh, *Org. Lett.* **1999**, *1*, 1513−1516. − [8b] T. Vilaivan, C. Khongdeesameor, P. Harnyuttanakorn, M. S. Westwell, G. Lowe, *Bioorg. Med. Chem. Lett.* **2000**, *10*, 2541−2545.
[9] A. Püschl, T. Tedeschi, P. E. Nielsen, *Org. Lett.* **2000**, *2*, 4161−4163.
[10] A. Püschl, T. Boesen, G. Zuccarello, O. Dahl, S. Pitsch, P. E. Nielsen, *J. Org. Chem.* **2001**, *66*, 707−712.
[11] [11a] G. Lowe, T. Vilaivan, *J. Chem. Soc., Perkin Trans. 1* **1997**, 539−546. − [11b] G. Lowe, T. Vilaivan, *J. Chem. Soc., Perkin Trans. 1* **1997**, 547−554.
[12] C. M. Topham, J. C. Smith, *J. Mol. Biol.* **1999**, *292*, 1017−1038.
[13] C. Gros, N. Galéotti, R. Pascal, P. Jouin, *Tetrahedron* **1999**, *55*, 11833−11842.
[14] T. Wöhr, F. Wahl, A. Nefzi, B. Rohwedder, T. Sato, X. Sun, M. Mutter, *J. Am. Chem. Soc.* **1996**, *118*, 9218−9227.
[15] A. Wittelsberger, M. Keller, L. Scarpellino, L. Patiny, H. Acha-Orbea, M. Mutter, *Angew. Chem. Int. Ed.* **2000**, *39*, 1111−1115.
[16] M. Pátek, B. Drake, M. Lebl, *Tetrahedron Lett.* **1995**, *36*, 2227−2230.
[17] P. N. Confalone, G. Pizzaloto, E. G. Bagglioni, D. Lollar, M. R. Uskokovic, *J. Am. Chem. Soc.* **1977**, *99*, 7020−7026.
[18] K. L. Dueholm, M. Egholm, O. Buchardt, *Org. Prep. Proced. Int.* **1993**, *25*, 457−461.
[19] [19a] H. T. Nagasawa, D. J. W. Goon, F. N. Shirota, *J. Heterocycl. Chem.* **1981**, *18*, 1047−1051. − [19b] W. Ando, Y. Igarashi, L. Huang, *Chem. Lett.* **1987**, 1361−1364.
[20] M. Egholm, O. Buchardt, P. E. Nielsen, R. H. Berg, *J. Am. Chem. Soc.* **1992**, *114*, 1895−1897.
[21] M. Schnölzer, P. Alewood, A. Jones, D. Alewood, S. B. H. Kent, *Int. J. Protein Res.* **1992**, *40*, 180−193.
[22] E. E. Baird, P. B. Dervan, *J. Am. Chem. Soc.* **1996**, *118*, 6141−6146.
[23] L. Christensen, R. Fitzpatrick, B. Gildea, K. H. Petersen, H. F. Hansen, T. Koch, M. Egholm, O. Buchardt, P. E. Nielsen, J. Coull, R. H. Berg, *J. Peptide Sci.* **1995**, *3*, 175−183.
[24] [24a] M. Egholm, L. Christensen, K. L. Dueholm, O. Buchardt, J. Coull, P. E. Nielsen, *Nucleic Acids Res.* **1995**, *23*, 217−222. − [24b] E. A. Lesnik, L. M. Risen, D. A. Driver, M. C. Griffith, K. Sprankle, S. M. Freier, *Nucleic Acids Res.* **1997**, *25*, 568−574.
[25] [25a] S. C. Brown, S. A. Thomson, J. M. Veal, D. G. Davis, *Science* **1994**, *265*, 777−780. − [25b] L. Betts, J. A. Losey, J. M. Veal, S. R. Jordan, *Science* **1995**, *270*, 1838−1841. − [25c] M. Eriksson, P. E. Nielsen, *Nature Struct. Biol.* **1996**, *3*, 410−413. − [25d] H. Rasmussen, J. S. Kastrup, J. N. Nielsen, J. M. Nielsen, P. E. Nielsen, *Nature Struct. Biol.* **1997**, *4*, 98−101.

[26] [26a] O. Almarsson, T. C. Bruice, J. Kerr, R. N. Zuckermann, *Proc. Nat. Acad. Sci. USA* **1993**, *90*, 7518−7522. − [26b] O. Almarsson, T. C. Bruice, *Proc. Nat. Acad. Sci. USA* **1993**, *90*, 9542−9546. − [26c] A. R. Scrinivasan, W. K. Olson, *J. Am. Chem. Soc.* **1998**, *120*, 492−499. − [26d] S. Sen, L. Nilsson, *J. Am. Chem. Soc.* **1998**, *120*, 619−631. − [26e] G. Shields, C. A. Laughton, M. Orozco, *J. Am. Chem. Soc.* **1998**, *120*, 5895−5904. − [26f] R. Soliva, E. Sherer, F. J. Luque, C. A. Laughton, M. Orozco, *J. Am. Chem. Soc.* **2000**, *122*, 5997−6008.

[27] G. M. Sheldrick, *SHELXS86, Program for the solution of crystal structures*, Univ. of Göttingen, Federal Republic of Germany, **1986**.

[28] D. J. Watkin, C. K. Prout, R. J. Carruthers, P. Betteridge, *CRYSTALS*, Chemical Crystallography Laboratory, Oxford, U.K., **1996**, issue 10.

[29] D. T. Cromer, *International Tables for X-ray Crystallography*, Kynoch Press, Birmingham, U.K., **1974**, vol. IV.

[30] J. R. Carruthers, D. J. Watkin, *Acta Crystallogr., Sect. A* **1979**, *35*, 698−699.

[31] D. J. Watkin, C. K. Prout, L. J. Pearce, *CAMERON*, Chemical Crystallography Laboratory, Oxford, U.K., **1996**.

Received March 2, 2001
[O01102]